Proceedings of ICRC 2001: 1129 © Copernicus Gesellschaft 2001

ICRC 2001

A method to detect UHE Neutrinos with AMANDA

S. Hundertmark[1], **for the AMANDA Collaboration**[2]

[1]Dept. of Physics, UC Irvine, Irvine, CA 92612, USA

[2]For a full author list see end of this volume

Abstract. This paper describes a method to detect UHE neutrinos with AMANDA. At energies $>10^{16}$ eV the earth becomes increasingly opaque to neutrinos. Because of the limited overburden above AMANDA, most of the UHE neutrino induced muons are expected from the horizon. The main challenge is the rejection of the large flux of downgoing atmospheric muon events, while retaining a large efficency for neutrino events.

1 Introduction

The main purpose of a large volume neutrino telescope is the identification of astrophysical neutrino sources. Sources may be point like or diffuse. The probability to detect a muon produced in a muon-neutrino interaction depends on the angle of incidence of the neutrinos. The distance traveled by a muon can not exceed the column density of matter availible for the neutrino interaction. Neutrinos above $\sim 10^{16}$ eV are strongly absorbed by the earth. Therefore UHE muons from neutrino interaction are mostly coming from the horizontal direction. Figure 1 shows that above E_ν=10^{16} eV downgoing neutrino-induced muon fluxes from various models exceed the background of downgoing atmospheric muons (including contribution from charm), which dictates the threshold for this analysis. Downgoing muon events of lower energy which resemble a signal event (i.e. muon bundles) are rejected using event information. Discovery of an UHE neutrino signal requires a detailed understanding of the simulation and detector. One example of the difficulties encounterd is the simulation of the background of downgoing muons. The compositon of the primary particle flux above the knee ($\sim 2 \cdot 10^{15}$ eV) is uncertain (see Freudenreich et al. (1990)). The amount of the contribution from the decay of charmed messons presents another uncertainty (Costa and Salles (2001)) and the air shower program Corsika (Heck (1998)) does not simulate charmed events. On the other hand, this creates an opportunity for AMANDA. The detection of the background from charm decays would provide an important constraint on the charm production.

Correspondence to: hundert@hep.pdf.uci.edu

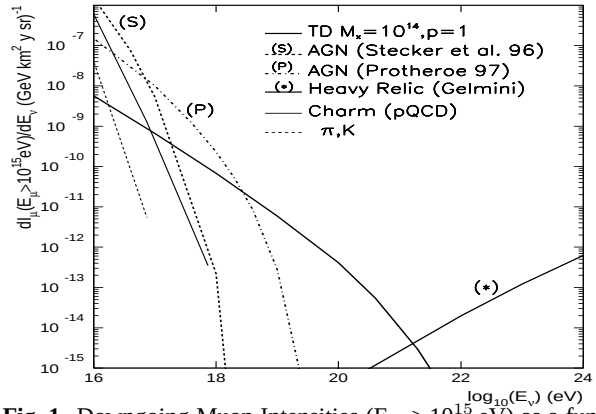

Fig. 1. Downgoing Muon Intensities ($E_\mu > 10^{15}$ eV) as a function of neutrino energy, taking into account the limited overburden above AMANDA. For topological defects (Sigl et al. (1999)), two AGN models (Stecker and Salamon (1996) and Protheroe (1997)), superheavy relics (Gelmini and Kusenko (2000)), a large charm prediction (Misaki et al. (1999)) and pion and kaon decays (Gaisser (1990)).

2 Method

To demonstrate the ability to reject the atmospheric muon background, while retaining a large effective area ($A_{\rm eff}$) for neutrinos we use several MC data sets and the experimental data itself. The analysis applies several cuts and a neural net (NN), enriching the data sample with events that resemble simulated UHE neutrino events. No reconstruction is used, as the AMANDA reconstruction tools were developed for low energy events and have a poor angular resolution for bright or distant events. Instead global event properties and timing information is used to distinguish between downgoing atmospheric muon and neutrino-induced events. One powerful rejection criteria is based on the idea that bright signal events have fewer OMs with only a single photon. At

UHE energies the flux of photons emitted by the muon is detectable over large distances. The arrival time distrubution is broad ($\sim$ few μs). This and the possibility for separated photons to create afterpulses generates multiple hits per OM.

3 The Detector

This analysis used data collected with AMANDA-B10 in 1997. This array consists out of 302 Optical Modules (OMs) deployed between 1500 m and 2000 m depth. A more detailed description of the detector and its basic characteristics can be found in Andres et al. (2001).

4 The Data Samples

4.1 Monte Carlo

Signal has been generated using single muons with energies equally distributed in $\log(\mathrm{E}_\mu)$ between 10^{12-20} eV and $\cos(\mathrm{zenith})$. The origin of the simulated muon track was uniformly distributed on a plane with a radius of 1000 m, located 500 m from the center of the detector. Propagation of the muons through the ice used the tracking code of Lipari (1991). This program allows tracking of muons up to 10^{20} eV. Atmospheric muon background was generated with Corsika. The relative abundances of cosmic ray primaries was taken from Wiebel-Sooth and Biermann (1999). The standard AMANDA downgoing muon sample was propagated with the code from Lohmann et al. (1985). The livetime of this sample corresponds to 0.48 days (normalized to the primary flux). Figure 2 shows the distribution of the primary energies for the different levels (as explained below). Using this figure, the minimum threshold for the primary energy was raised from 0.8 TeV to 80 TeV (biased sample). This enables the generation of a larger number of events. Propagation was done with Lipari. The knee in the primary cosmic ray spectrum has been simulated by weighting events with primary energies above 2×10^{15} eV according to a 0.3 steeper spectrum. The relative abundance of the primaries was not changed. The livetime of this sample was $\sim$7.2 days.

4.2 Experimental Data

The 1997 high multiplicity sample (Number of hit channels (NCH) >100) as used in the monopole analysis (Niessen (2001)) was used. A small number of OMs experienced electronic malfunction in some runs. These runs were excluded from the current analysis. With 25 % dead time the integrated livetime was 75 days.

5 Event Selection

The event selection used several parameters, describing global event and time properties . The parameters are defined as:

F1H Fraction of hit channels with exactly one hit
NCH Number of hit channels
NH Number of hits for all channels
MA The mean amplitude for hit channels
SIGA The square root of the variance of the amplitudes

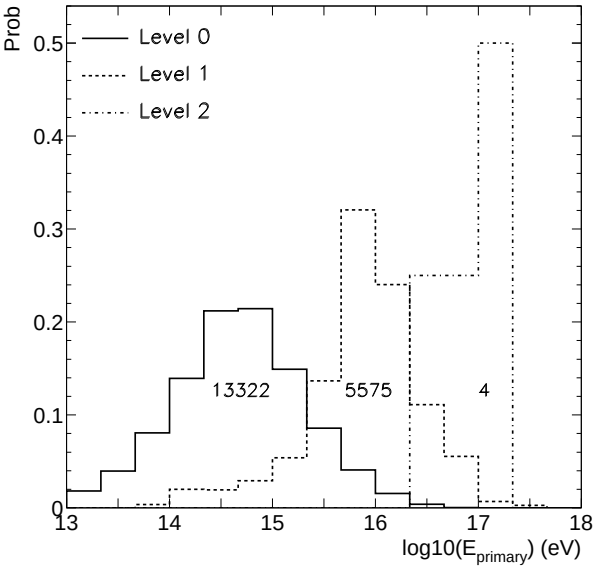

Fig. 2. The distribution of the energy of the primary for the Corsika simulation for the three levels as defined below. Level 0 is from the unbiased, while the other two are from the biased Corsika sample. Indicated are the unweighted number of events for each level.

SIGT The square root of the variance of the hit times
NN A neural net using the above variables

The selection of events was done in several steps:

1. Calibrating, cleaning of cross talk, cleaning of unstable OMs
2. Rejecting events with NCH$<$95
3. Rejecting events caused by electronic noise
4. Rejecting events with F1H$\geq$0.55
5. Rejecting events with NN$\leq$0.95

Steps 1–3 define level 0, step 4 defines level 1 and step 5 defines level 2.

Level		Experim.	Corsika	Cor. bias	MC Signal
0	Events	2405055	12906	60341*	25628
	Events/day	32067	26888	8381*	-
1	Events	19584	473	4065	21203
	Events/day	261	985	565	-
2	Events	9	-	0.89 (4)	18477
	Events/day	0.12	-	0.12	-

Table 1. Absolute numbers and event rates per day for the experimental data, Corsika MC (0.48 days livetime), "biased" Corsika (7.2 days livetime) and E^{-1} Signal. (4) gives the number of unweighted MC events. The numbers with * were generated with the higher threshold and are not comparable with the others in this line.

5.1 Level 0

After steps 1 to 3 the initial high multiplicity sample is reduced to $\sim$30 % or $\sim 2.4 \times 10^6$ events. Table 1 shows the event rate per day of the Corsika MC in agreement with the experimental data. Figure 3 shows the multiplicity distribution (NCH) for the experiment, the Corsika MC and the

MC signal. Agreement between the background MC and the experimental distribution is seen. The UHE neutrino-induced muons tend to have a higher multiplicity than the atmospheric muons.

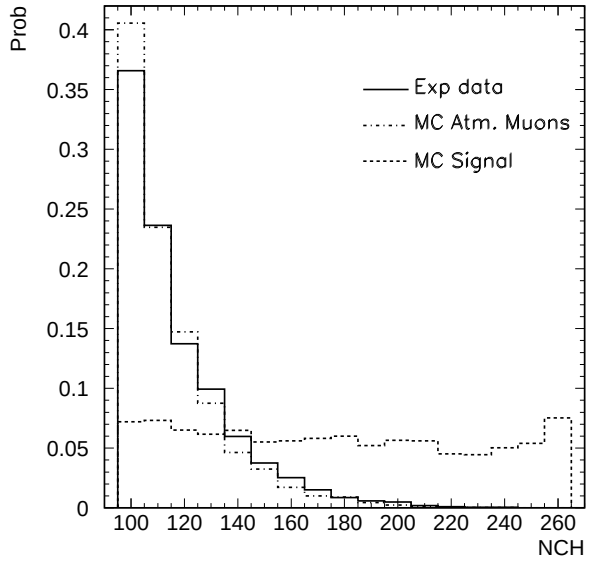

Fig. 3. NCH distribution for experiment, Corsika and signal MC.

5.2 Level 1

The AMANDA Data Aquisition has the capability to record several photon arrival times (hits) per OM . Figure 4 shows the distribution of F1H at level 0. The experimental data and the downgoing muon MC are well seperated from the signal MC. Keeping events with F1H$<$0.55, reduces the experimental data to less than 1 % of the level 0, while 83 % of the signal survives. An overestimation of the afterpulse probability shifts the Corsika MC compared to the experimental data, explaining the higher passing rate of 3.7 %.

5.3 Level 2

A neural net (Schwindling et al. (1999)) was trained with a small fraction of the biased Corsika and the signal MC. The six variables defined above were used as input. The F1H variable was re-evaluated without afterpulses. Figure 5 shows the output of the NN. Most of the experimental data and the Corsika MC events were identified as background (NN close to 0.). The shape is in good agreement. Rejecting events with NN$\leq$0.95 results in a rate of 0.12 events/day for the experiment and the Corsika MC (see table 1). The remaining Corsika events have a mean number of muons of 661, compared to 42 at level 0. The summed muon energy per event increased from 6×10^{13} eV to 10^{15} eV. This shows that remaining background at this level consists of large muon bundle events. Figure 6 shows that $A_{\rm eff}^{\rm level\,2}$ is $\sim$0.3 km^2 for horizontal events above 10^{18} eV. The area for vertical downward going muons is $\sim$30 % lower. A signal efficency of $\epsilon = A_{\rm eff}^{\rm level\,2}/A_{\rm eff}^{\rm trigger}$ $\sim$0.4 has been achieved.

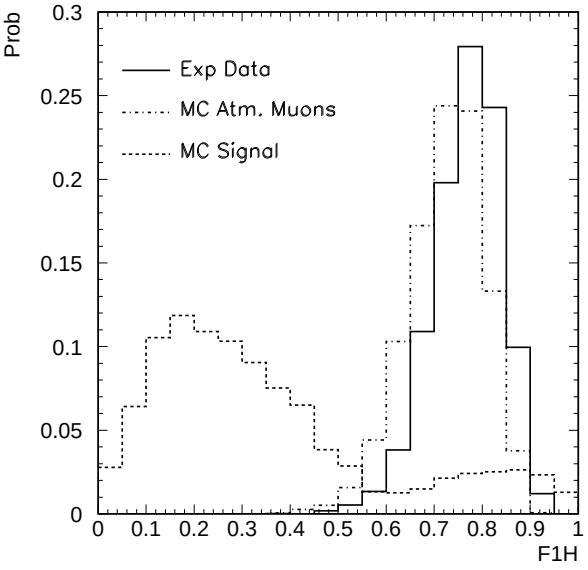

Fig. 4. The fraction of hit modules with exactly one hit.

6 Signal Expectation

Following Alvarez-Muniz and Halzen (2001) we computed the number of events per year from the sources shown in figure 1. A muon threshold of 10^{15} eV was introduced. The finite ice overburden was taken into account. The detector area ($A_{\rm eff}$) from figure 6 (level 2) was evaluated at the energy of the muon at the detector. Of $\mathcal{O}$(5-10) events per year are expected from the different sources in AMANDA-B10 (see table 2).

AGN (Stecker)	AGN (Protheroe)	Relics (Gelmini)	Charm (pQCD)
16	5	10	14

Table 2. Number of events expected per year for AMANDA-B10 at level 2 for the sources shown in figure 1.

7 Discussion, Conclusions and Outlook

The application of a simple cut and a neural net based on global event and timing information rejected most of the experimental events for a livetime of 75 days. The remaining events are consistent with being background events. The trigger area reaches 1 km^2 for horizontal muons with $E_\mu \approx 10^{20}$ eV. The investigation outlined in this paper produced a signal efficency of $\sim$0.4. Because of the uncertainties in the simulation chain the agreement between experimental data and atmospheric muon MC is acceptable. Most of the uncertainties are related to the energy regime in this analysis. For the neutrinos the charged current coss-section is uncertain by a factor of $\sim 2^{\pm 1}$ (Gandhi et al. (1998)) at the energies of interest. The muon propagation is subject to uncertainties (cross-sections) and availible algorithms are not designed for these energies (e.g. the LPM effect is not included).

The detector hardware was not designed to accomodate the

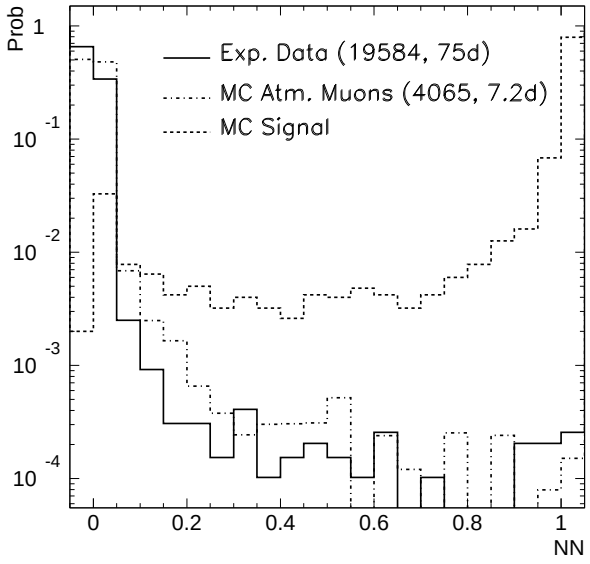

Fig. 5. The NN output for events on level 1.

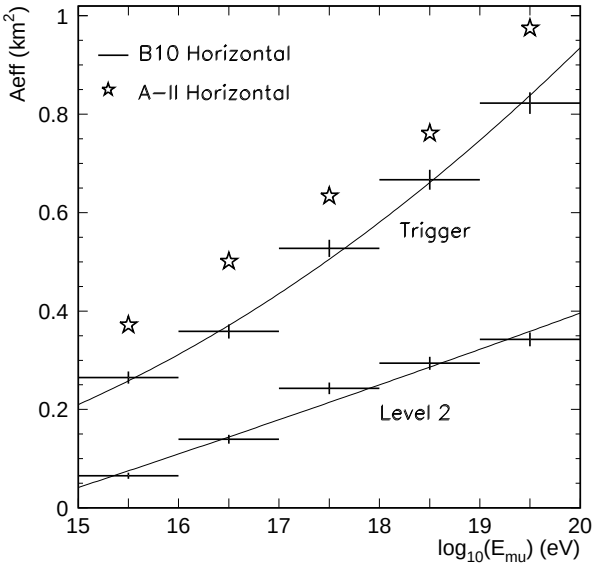

Fig. 6. A_{eff} for signal events on the trigger level and level 2. The crosses are for AMANDA-B10, while the stars indicate the tigger area for AMANDA-II.

large amount of photons induced by bright events. Information is lost or degraded by electronic limitations. The detector simulation was extended to simulate this. In the absence of a known source of comparable energy, the calibration of the detector response is difficult. To adress this problem the MC response to large energy deposits was studied and compared to data taken *in situ* with the N_2-Laser.

The investigation presented here is selecting events of higher energies. Therefore this study may be sensitive to the composition and the spectral slope of the elements above the knee. We have investigated one model as discussed in Freudenreich et al. (1990). The change to a different model will affect the MC background expectation. A better description of the afterpulse probability in the detector MC will improve the agreement in the F1H variable at level 0. The development of further selection criteria to reject atmospheric muons after level 2 is currently limited by the background MC (4 events after level 2). A new MC production will remedy this situation.

For AMANDA-II (for a description see Wischnew (2001)) the trigger area increases by $\sim$20 % (as shown in figure 6). Because AMANDA-II has more than twice the number of OMs, the signal efficency is expected to increase compared to AMANDA-B10. This and the analysis of the total $\sim$4.5 years of data recorded since 1997 will increase the integrated exposure significantly. It is expected that a limit that impacts models shown in figure 1 can be set or in the most optimistic case a signal can be identified.

Acknowledgements. This work was supported by DFG(Germany), NSF Physics Division (US) and AAS (US) International Travel Grant Program .

References

Alvarez-Muniz, J. and Halzen, F., Phys. Rev. D **63**, 037302 (2001) [astro-ph/0007329].
Andres, E. et al., Nature **410**, 441 (2001).
Costa, C. G.,and Salles, C., hep-ph/0105271.
Freudenreich, H. T. et al., Physical Review D, Vol 41, Number 9 (1990) 2732-2750.
Gaisser, T. K., *Cambridge, UK: Univ. Pr. (1990) 279 p.*
Gandhi, R. et al., Phys. Rev. D **58**, 093009 (1998) [hep-ph/9807264].
Gelmini, G., and Kusenko, A., Phys. Rev. Lett. **84**, 1378 (2000) [hep-ph/9908276].
Heck, D., Prepared for International Workshop on Simulations and Analysis Methods for Large Neutrino Telescopes, Zeuthen, Germany, 6-9 Jul 1998.
Lipari, P. and Stanev, T., Physical Review D 44 (1991) 3543-3554.
Lohmann, W., Kopp, R. and Voss, R., Cern 85-03 (1985).
Misaki, A. et al., hep-ph/9905399.
Niessen, P. et al., these proceedings.
Protheroe, R. J., ASP Conf. series, Vol 121, pp585–588 (1997) [astro-ph/9607165].
Protheroe, R. J. , Nuclear Physics B (Proc. Suppl.) 77 (1999) 465-473.
Schwindling, J., Mansouli, B. and Couet, O., `http://wwwinfo.cern.ch/asd/paw/mlpfit/pawmlp.html`
Sigl, G., Lee, S., Bhattacharjee, P. and Yoshida, S., Phys. Rev. D **59**, 043504 (1999) [hep-ph/9809242].
Wiebel-Sooth, B., Biermann, P., Landolt-Bornstein, Vol. VI/3c, Springer Verlag (1999) 37-90.
Wischnew, R. et al., these proceedings.
Stecker, F. W. and Salamon, M. H., Space Sci. Rev. **75**, 341 (1996) [astro-ph/9501064].